Electromagnetic modelling of foetus and pregnant woman exposed to extremely low frequency electromagnetic fields

C. Gonzalez[1], A. Peratta[1] & D. Poljak[2]
[1]*Wessex Institute of Technology, UK*
[2]*University of Split, Croatia*

Abstract

The paper presents a three dimensional BEM model of a pregnant woman and foetus exposed to extremely low frequency electromagnetic fields. In particular, the case scenario solved is focused on the case of exposure to high voltage power transmission lines. The paper presents the corresponding theory, BEM computational implementation, and results. The latter are expressed in terms of current density, potential and electric field in the different tissues. This work is part of an ongoing research whose overall objectives are to provide accurate estimations of fields and induced currents for assessing exposure of human bodies to electro-magnetic fields.
Keywords: pregnant woman; boundary element method; electric field.

1 Introduction

Exposure levels in the foetus of a pregnant woman are difficult to estimate mainly because of the following three main factors. Firstly, the lack of data on electrical properties at low frequency for the foetus and the surrounding tissues; secondly, the impossibility of collecting *in-vivo* measurements in a real case scenario; and finally, because of the complicated changing geometrical and physical properties of the body along the pregnancy period. Hence, a numerical modelling approach is highly appealing, especially for conducting sensitivity analysis on the electrical properties, which are scarce and scattered in the available literature.

The aim of this paper is to analyse the case of exposure of a pregnant woman to high voltage overhead power-lines by means of a collocation BEM based on an three dimensional anatomical model of the mother and foetus.

WIT Transactions on Modelling and Simulation, Vol 47, © 2008 WIT Press
www.witpress.com, ISSN 1743-355X (on-line)
doi:10.2495/BE080091

The developed code will be used for measuring induced currents and electric fields in the foetus in different scenarios of conductivities at different time stages of pregnancy, and considering different presentations of the foetus inside the maternal matrix. The different stages of pregnancies relevant for the modelling arise not only from the geometrical point of view but also due to the variation of electrical properties of tissues during gestation [1].

In time harmonic EM fields, Maxwell equations can be decoupled when the characteristic size of the model (2 m for the whole human body) is much smaller than the characteristic vacuum wavelength ($\lambda_0 \sim 860$ m at frequency $\nu = 350$ kHz) and the displacement currents can be neglected in comparison to the resistive ones. Therefore, the high voltage LF approach is applicable and the numerical problem summarises into solving the non-homogeneous Laplace equation.

On the other hand, the Boundary Element Method (BEM) [2, 3] is a well established numerical technique which provides accurate solutions in complex geometries. The beauty of BEM is that it takes into account the fundamental solution of the leading partial differential operator, and that the discretisation can be done only in the boundary of the problem. The BEM has been successfully applied for solving problems of biological tissues, other than the human eye, exposed to low and high frequency electromagnetic (EM) fields [4–7].

2 Low frequency EM modelling with boundary elements

When considering biological tissue exposure to high voltage and low currents the most influential field is the electric one. Assuming both conductivity σ and permittivity ε to be constant within a finite region of interest (sub-domain) it is derived from Maxwell's equations that the electric scalar potential φ obeys the non-homogeneous Laplacian-type equation: $\nabla \cdot [(\sigma + i\omega\varepsilon)\nabla\varphi] = 0$, where $e^{i\omega t}$-time dependency convention has been used, being $\omega = 2\pi\nu$ the angular frequency of the incident field, ε the permittivity, and $i^2 := -1$. The corresponding integral equation [2, 3] for the potential $\varphi(\mathbf{x_s})$ in a homogeneous domain is:

$$c_i\varphi(\mathbf{x}_i) + \int_\Gamma \frac{\partial G^*(\mathbf{x}, \mathbf{x}_i)}{\partial \hat{n}}\varphi(\mathbf{x})d\Gamma - \int_\Gamma G^*(\mathbf{x}, \mathbf{x}_i)\frac{\partial \varphi}{\partial \hat{n}}(\mathbf{x})\, d\Gamma = 0, \qquad (1)$$

where Ω is the integration domain with boundary $\Gamma = \partial(\Omega)$ of outward unit normal $\hat{\mathbf{n}}$, G^* is the Green's function of Laplace equation: $\nabla^2 G^* + \delta(\mathbf{x}_i, \mathbf{x}) = 0$, and $\partial G^*/\partial\hat{n}$ its normal derivative in $\hat{\mathbf{n}}$ direction. Also, proper boundary conditions are applied to $\Gamma = \partial(\Omega)$, i.e. Dirichlet, Neumann or Robin type. In 3D space the Green's function becomes $G^* = 1/(4\pi r)$ where $\mathbf{r} = \mathbf{x} - \mathbf{x}_i$, $r = |\mathbf{r}|$ is the distance between the field ($\mathbf{x} \in \Gamma$) and source ($\mathbf{x}_i \in \Omega$) points, and c_i is a constant dependent on the Cauchy principal value integration of the singularity at the source point. Discretisation with constant elements of eq. (1) yields:

$$c_i\varphi_i + \sum_{j=1}^{N_e} H_{ij}\varphi_j - \sum_{j=1}^{N_e} G_{ij}E_{n,j} = 0, \qquad (2)$$

where φ_j and $E_{n,j}$ denote potential and normal electric field, respectively in j-th element, and **G** and **H** are the usual BEM single and double layer integrals [3], respectively. The assembly of (1) leads to a linear system of algebraic equations $\mathbf{Ax} = \mathbf{b}$, whose solution provides the unknown φ and E_n values at the boundary. At LF, biological tissues behave as good conductors with conductivity values of the order of 0.5 S/m, and electric permittivity 10^{-10} F/m , i.e. $\varepsilon_r \sim 100$; and the air represents a nearly perfect dielectric. In addition, air has negligible conductivity in comparison with tissues, and the permittivity of most biological tissues is few orders of magnitude greater than ε_0 [8]. Therefore, appropriate matching conditions between air (0) and tissue (1,2) and different tissues, can be written as:

$$\left[\sigma \frac{\partial \varphi_I}{\partial n}\right]_{1,2} = \left[\omega\varepsilon \frac{\partial \varphi_R}{\partial n}\right]_0 \quad ; \left[\sigma \frac{\partial \varphi_I}{\partial n}\right]_1 = \left[\sigma \frac{\partial \varphi_I}{\partial n}\right]_2, \tag{3}$$

respectively; where $\mathbf{j} = -\sigma \nabla \varphi$ is current density and $\mathbf{j} \cdot \hat{\mathbf{n}}$ is preserved.

3 Physical model

The physical model involves two challenging aspects, the changing geometrical and physical data of the relevant tissues for mother and foetus. Different stages of pregnancy are modelled separately in order to consider the changes throughout gestation. These changes are related not only to the volume, mass and geometry of the maternal body and foetus, but also to the electrical properties of the participating tissues.

The background information for foetal and embryo development was obtained from ref. [9]. The embryonic period (3^{rd} to 8^{th} weeks) is the time when all internal and external structures develop in the embryo. During this critical period, the exposure of an embryo to certain agents such as external electromagnetic fields may cause major congenital malformations.

The end of the embryonic stage occurs by the end of eighth week and then the foetal period begins. During the fetal period, the growth, development and maturation of the structures that have been already formed takes place. The definition of the model in this work reflects the four different stages of pregnancy spread along gestation, and the timing correspond to the 8^{th}, 13^{th}, 26^{th} and 38^{th} gestational weeks.

The conductivity data for the foetus is scarce and scattered in the literature. For the maternal abdomen, the division into sub-domains is based on the different properties of the tissues. The amniotic fluid (AF) has the highest conductivity which varies depending on the period of gestation [1,8]. Kidney, muscle bone cortical, bladder, spleen, cartilage and skin have all conductivity values very close to 0.1 S/m, ovary and cartilage have conductivity $\sim$ 0.2 S/m. Therefore, all these tissues can be grouped into one sub-domain, namely maternal tissue. The uterus conductivity is 0.23 S/m, which is very similar to the conductivity of the maternal tissue. According to ref. [1], the placenta is assumed to have the same conductivity as the blood. and considered as part of the maternal-tissue sub-domain.

Consequently, the maternal abdomen is divided into three sub-domains namely "maternal tissue", "amniotic fluid", contained within the uterus, and "foetus".

The geometrical information for the foetus model was built with the help of CT images at different stages [10] and data on the anatomy of the mother and foetus were extracted from [11]. The anthropometric measurements for the size of the foetus are based on the crownrump length (CRL), and the biparietal diameter (BPD) [11], whose growth is almost linear in the early weeks of pregnancy, but there is a progressive reduction in growth rate, especially during the final weeks. Reference values of the surface area of the foetal body [11] were also adopted for defining the model. During the foetal period length and weight do not change in the same way. Foetal length change is greatest in the second trimester, while foetal weight change is greatest in the final weeks of development.

Furthermore, the foetus is free to move inside the maternal abdomen, principally until the 24^{th} week. Since then, the movement is more constrained. In obstetrics, the foetal orientation and position are normally described in terms of the *foetal lie, presentation attitude* and *position*. The *foetal lie* describes the orientation of the longitudinal axe of the foetus in relation to the longitudinal axe of the mother. If the longitudinal axe of the foetus is parallel to the longitudinal axe of the mother, the foetus is in *longitudinal lie*, while if it is perpendicular or oblique, the foetus is in *transverse* or *oblique lie* respectively. Longitudinal lie occurs in the 95% of the cases.

The fetal attitude describe the relative position of different parts of the body of the foetus in relation with his own body. For example, in the most normal fetal attitude, referred as well as *the fetal position*, the head is tucked down to the chest, with arms and legs drawn in towards the centre of the chest.

The *presentation* of the foetus refers to his orientation in relation with the birth channel. The normal presentation is cephalic, with the head oriented to the birth channel. When the foetus is in cephalic presentation and fetal position, then the presentation is referred to as *vertex presentation*. This presentation is the most common at delivery and occurs in the 96% of the births. Another presentation that occurs in the 3.5% of the births is the *breech presentation* when the buttocks are oriented towards the birth channel. The last and less frequent presentation (0.5%) is the *shoulder presentation* associated with transverse lie.

Figure 1 shows a view of the model developed for the 26 weeks foetus in the cephalic and breech presentations and a general 3D view of one of the models (1.7 m tall) at 26 weeks of pregnancy with the foetus in cephalic presentation. The data for the maternal geometry and its variation along pregnancy was obtained from [11]. Roughly, during gestation there is a change in the volume of AF, and a general increase of mass distributed over the maternal body. Figure 1 shows a The scenarios in this work are prepared in order to study different scenarios of electrical conductivity (see Table 1), different time stages of pregnancy, and different presentations of the foetus.

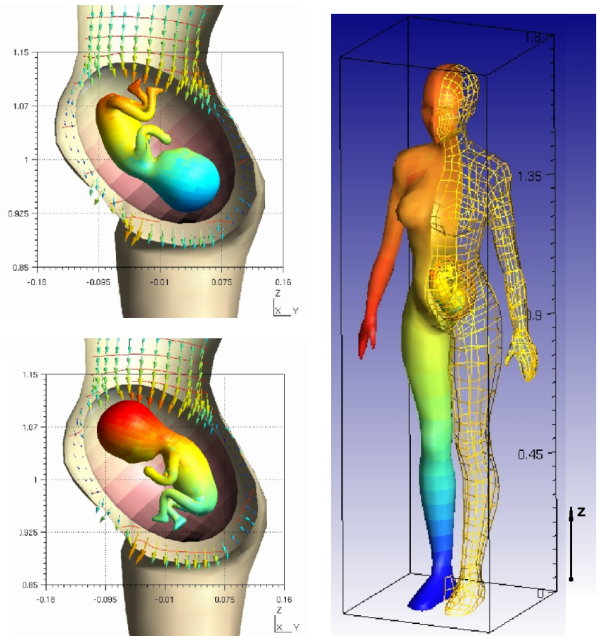

Figure 1: 3D view of the model at 26 weeks of pregnancy in cephalic presentation.

Table 1: Conductivity scenarios.

Scenario	[S/m]	Week 8	Week 13	Week 26	Week 38
	σ_f	0.23	0.23	0.23	0.23
1	σ_{AF}	1.28	1.28	1.27	1.10
	σ_m	0.20	0.20	0.20	0.20
	σ_f	0.996	0.996	0.574	0.574
2	σ_{AF}	1.70	1.70	1.64	1.64
	σ_m	0.52	0.52	0.52	0.52
	σ_f	0.732	0.732	0.396	0.396
3	σ_{AF}	1.70	1.70	1.64	1.64
	σ_m	0.17	0.17	0.17	0.17

4 Numerical implementation

The maternal body is placed in an open environment, standing barefoot on a perfectly conductive infinite flat surface at $z = 0$, at ground level ($\varphi = 0$.) This represents the worst case scenario for open environments in which currents throughout the body are expected to be maximum.

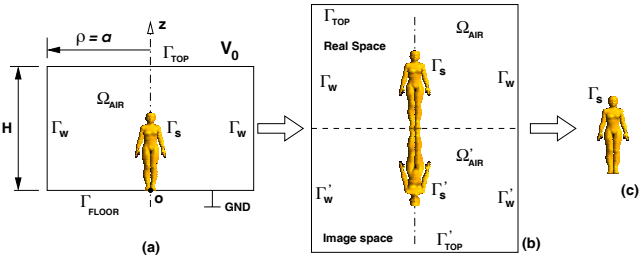

Figure 2: Simplification of the conceptual model. (a) Original. (b) Floor discretisation is avoided by reflecting the problem. (c) Top and lateral wall discretisation is replaced with asymptotic analytical integrations.

The pregnant woman is exposed to a reference field oriented in z direction, with asymptotic value $E_0\hat{\mathbf{z}}$ when $z \to \infty$, as shown in Figure 2. These conditions are recreated by fixing an equi-potential plane $\varphi = V_0$ at $z = H$, where H is sufficiently larger than the height of the woman, and then scaling up the results by a factor $\theta = H/V_0 \times E_0$, in order to translate the results into a particular magnitude of incident field E_0. The assumptions involved have helped to elaborate a particular BEM implementation which reduces dramatically the number of degrees of freedom in the calculation in comparison to the direct BEM application. Thus, the BEM for this work considers a symmetry plane at the ground level, lateral boundary walls located at infinity, and constant potential at a height h enough far away from the model. With these assumptions, only the interfaces between different tissues in the human body and the outer skin in contact with the air around need to be discretised. In this way the mesh discretisation of the external domain including soil, lateral walls and ceiling were eliminated. Figure 2 illustrates the conceptual model developed under these assumptions. The integrals on lateral, top and bottom surfaces of the bounding box in the model were replaced by an equivalent source term: $-zV_0/H$, added to the right hand side member of (1), where z is the vertical coordinate of the source point $\mathbf{x}_i$, V_0 is the potential imposed on the top surface, and H the height of the model. The results in this paper were obtained by adopting $V_0 = 1$ V and $H = 5$ m (i.e. to translate the results to the case of $E_0 = 10$ kV/m, a scaled factor $\theta = 5 \times 10^7$ for $\mathbf{j}$ is adopted in order to obtain $\mathbf{j}$ in mA/m^2).

The model consists of four sub-domains, Ω_{AIR}, Ω_{BODY}, Ω_{AF} and Ω_{F}, namely air, body, AF and foetus, respectively. The air is bounded by Γ_{TOP}, Γ_{W}, Γ_{FLOOR} and Γ_S; while the body is bounded by Γ_{S} and Γ_{ti}, $i = 1, \ldots, N_t$, where Γ_{ti} represents the surface enclosing the different internal organs embedded in the homogeneous body, and N_t is the number of organs. Part of Γ_S is in contact to the ground Γ_{SF}, while the rest is in contact to the air Γ_{SA}.

Table 2 summarises the relationship between sub-domains, surfaces and boundary conditions in the model. The complete problem involves the air (considered as an external problem), and the body with its internal organs and the foetus. In order to reduce the computational burden, the BEM solving approach is split into

Table 2: Connectivity between sub-domains and surfaces, and boundary conditions. "×" symbol indicates an unknown of the problem while "-" symbol indicates that the corresponding surface is not related to the sub-domain.

	Ω_{AIR}		Ω_{BODY}		Ω_{AF}		Ω_{F}	
	φ	E_n	φ	E_n	φ	E_n	φ	E_n
Γ_{TOP}	V_0	×	-	-	-	-	-	-
Γ_{W}	$\frac{zV_0}{H}$	0	-	-	-	-	-	-
Γ_{FLOOR}	0	×	-	-	-	-	-	-
Γ_{SA}	×	×	×	×	-	-	-	-
Γ_{SF}	-	-	0	×	-	-	-	-
Γ_{T1}	-	-	×	×	×	×	-	-
Γ_{T2}	-	-	-	-	×	×	×	×

two stages: external and internal. In the external stage the air coupled to the homogeneous body is solved, obtaining as a result the electric field and potential in the skin, which are imposed as input boundary conditions in the second stage in order to solve the interior problem of the human body, consisting of several subdomains. The inclusion of the body without internal tissues does not introduce significant errors in the results on the skin.

5 Results and discussion

Figure 3 shows a lateral view of the sliced model of the pregnant woman. The direction of the electric field in the maternal tissues is shown with black arrows. The iso-lines represent the electric potential field. Figure 4 shows a 3D view of the sliced model of the pregnant woman including some of the results obtained for the potential and electric field. The model is partially sliced with clipping planes in order to visualise the interior results. There are seven colorbars on the left hand side of the figure which show the correspondence between the colormap and the numerical scale in each case. All results correspond to the case of exposure to 1/5 V/m. "U_body0" corresponds to the potential observed inside the model in the sagittal plane, excluding the limbs. "U_Foetus" refers to the potential measured in the skin of the foetus, the values range from 1.41 μV to 1.34 μV. "U_Skin" corresponds to the potential measured in the maternal skin, i.e. the interface between air and body. The maximum value $\sim$ 2 μV is obtained near the head, while the minimum ($\sim O(10^{-3}\ \mu\text{V})$) is in the nearest part of the skin contacting the soil (feet). "E_body" and "E_body0" correspond to the vector field plot representing the electric field in the internal part of the maternal body. The former, ranging from 0.74 μV/m to $\sim$ 0.02 μV/m, refers to the coronal sectioning plane including arms and legs, while the latter, ranging from $\sim$ 2 μV/m to $\sim$ 0.02 μV/m refers to the sagittal planes excluding limbs. Finally, "U_Uterus" and "U_Body" indicate the

potential in the uterus and body surfaces, respectively. It can be observed how the uterus tends to concentrate the field lines. This is because of its higher conductivity with respect to the maternal tissue. Figure 4(right) illustrates the observation line that goes along the spine of the foetus, where the current density has been measured. The summary of current density results ($j = |-\sigma_f \nabla\varphi|$), for an incident electric field of 10 kV/m, obtained for 24 models involving cephalic and breech presentations, conductivity scenarios 1, 2, and 3 and four gestational periods can be observed in Figure 5. shows the mean, maximum and minimum values of current density computed in the foetus at different weeks of pregnancy for different conductivity scenarios and foetus presentations. The trend is that the maximum current appears at the 8^{th} gestational week, then it decreases progressively as the foetus develops. This decrease can be explained as a consequence of the two following factors. First, the foetus and AF conductivity decrease with age. Second, as the foetus grows, he tends to adopt a *vertex presentation* (extremities drawn in towards the centre of the chest and head tucked down to the chest), hence his external surface is smoother and the cross sectional area becomes more regular.

In all conductivity scenarios the current density in breech presentation tends to be higher than in the cephalic. This effect is less pronounced in the last stage of pregnancy (38 week).

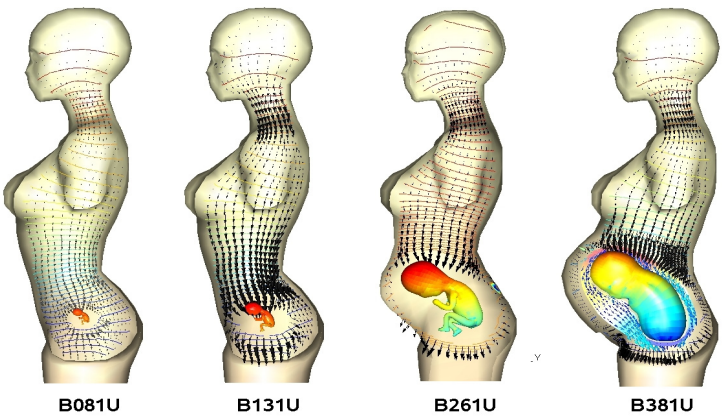

Figure 3: Lateral view of BEM models at 8, 13, 26 and 38 weeks (breech presentation).

Table 3: Dosimetry analysis.

	j_n [mA/m^2]			E_0 [kV/m] field restriction		
Scenario	1	2	3	1	2	3
Maximum	7.4	10.7	17	2.70	1.87	1.18
Typical	3.2	5.8	7.5	6.25	3.45	2.67

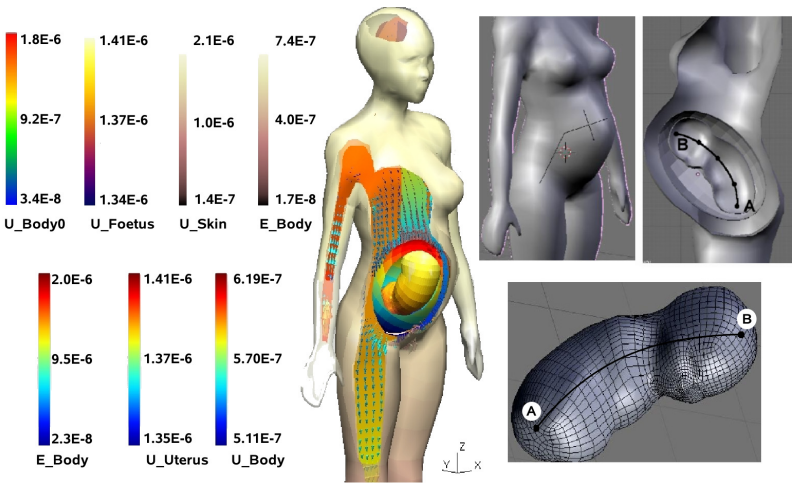

Figure 4: BEM model and exposure results (left). Observation line along the spine of the foetus.

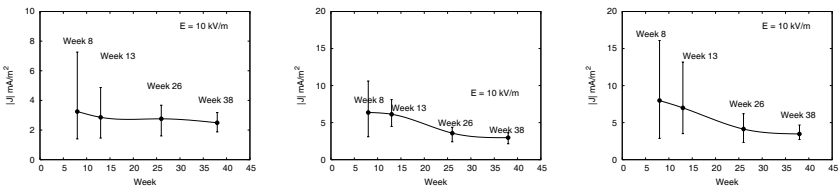

Figure 5: Mean current density calculated in the foetus at weeks: 8, 13, 26 and 38 of pregnancy for scenario 1 (left), 2 (middle), and 3 (right).

6 Summary and conclusions

The BEM has been successfully applied in order to calculate induced currents, potentials and electric fields in a three dimensional anatomical model of a pregnant woman exposed to a vertically incident ELF electromagnetic field. For fixed exposure, the maximum value of current density in the foetus occurs during the 8^{th} week. The maximum current density obtained in the foetus for an incident external field of 10 kV/m is 7.4 mA/m^2. On the other hand, the restriction recommended for public exposure by ICNRP [12] is 2 mA/m^2. Then, this restriction translates into a maximum external field $E_1 = 2.7$ kV/m. Table 3 generalises this analogy for the three scenarios studied by showing the equivalent electric fields restrictions. The first three columns indicate the current densities obtained in the foetus at week 8 for an incident electric field of 10 kV/m in the three different scenarios. The last three columns indicate the external electric field that should be applied in order to measure a current density of 2 mA/m^2 in the foetus. The first row corresponds to the maximum values while the second to the average ones. According to these

results, the mean values give a restriction for the electric field of approximately 3 kV/m based on the current circulating in the foetus, while the current restriction suggests approximately 50 kV/m, if it is based only on the maternal brain.

References

[1] P.J. Dimbylow. Development of pregnant female, hybrid voxel mathematical models and their application to the dosimetry of applied magnetic and electric fields at 50 hz. *Phys. Med. Biol.*, 51:2383–94, 2006.

[2] C. Brebbia, J. Telles, and L. Wrobel. *Boundary Elements Techniques*. Splinger-Verlag, Berlin, Heidelberg, New York and Tokio, 1984.

[3] C. Brebbia and J.Dominguez. *Boundary Elements, an Introductory Course*. Computational Mechanics Publications. McGraw-Hill, New York, Colorado, San Francisco, Mexico, Toronto, 2^{nd} edition, 1992.

[4] C. Gonzalez, A. Peratta, and D. Poljak. Boundary element modeling of the realistic human body exposed to extremely low frequency (elf) electric fields: Computational and geometrical aspects. *IEEE Trans. on Electromagnetic Compatibility*, 49(1):153–62, 2007.

[5] A. Peratta, C.Gonzalez, and D. Poljak. Geometrical aspects of 3d human body exposed to extremely low frequency electromagnetic fields. In *14th Int.Conf on Software, Telecomm and Comp. Networks. IEEE*, Split CROATIA, 2006.

[6] A. Peratta, C. Gonzalez, and D. Poljak. Current density induced in the human body due to power distributions lines using the BEM. *J. Comm. Soft. Syst.*, 3(1):11–16, 2007.

[7] A. Peratta. 3D Low frequency electromagnetic modelling of the human eye with boundary elements: Application to conductive keratoplasty. *Engineering Analysis with Boundary Elements*, 2008. To appear in 2008.

[8] S.Gabriel, R.W. Lau, and C. Gabriel. The dielectric properties of biological tissues: Ii. measurements in the frequency range 10 hz to 20 ghz phys. *Phys. Med. Biol.*, 41:2251–69, 1996.

[9] MJT FitzGerald MJT and M. FitGerald. *Human Embryology*. W. B Sauders Company, London, 1994.

[10] UNSW Embriology - Dr.Mark Hill. Website.

[11] ICRP 2002. Basic anatomical and physiological data for use in radiological protection: reference values. *ISNN 0146-6453*, 89, 2002.

[12] ICNIRP. Guidelines for limiting exposure to time-varying electric, magnetic, and electromagnetic fields (up to 300 ghz). *Health Physics.*, 74(4):494–522, 1998.